Original Article

Institution of MECHANICAL ENGINEERERS

Journal of SYSTEMS AND CONTROL ENGINEERING

Proc IMechE Part I: J Systems and Control Engineering
2024, Vol. 238(7) 1273–1284

DOI: 10.1177/09596518241233318
journals.sagepub.com/home/pii
Sage

Adaptive multi-dimensional Taylor network tracking control of time-varying delay nonlinear systems subject to input saturation

Lian-Lian Zhai[1], Shan-Liang Zhu[1,2] and Yu-Qun Han[1,2]

Abstract

For the tracking control problem of a class of nonlinear systems with input saturation constraint and time-varying delay, an adaptive tracking control scheme based on multi-dimensional Taylor network (MTN) is designed, and the proposed control scheme has the advantages of simple structure and small computation. A Gaussian error function is introduced to transform the input saturation into a linear model with bounded error. The Lyapunov-Krasovskii function is constructed, and the nonlinearity of the system is approximated using MTN, and an adaptive control strategy is constructed based on the backstepping method. The results show that the proposed control method can both ensure that all signals in the closed-loop system are bounded and achieve convergence of the tracking error to a small neighborhood near the origin. Numerical simulations verify the effectiveness of the method.

Keywords

Input saturation, time-varying delay, multi-dimensional Taylor network, nonlinear systems, adaptive control

Date received: 27 July 2023; accepted: 25 January 2024

Introduction

In recent years, the study on nonlinear systems have aroused broad concern due to its widespread application in engineering, and many tracking control schemes have been developed.[1,2] It should be pointed out that complex unknown uncertainties that inevitably exist in nonlinear system, which may lead to essential obstacles in controller design and stability analysis. Therefore, combining intelligent control methods, such as fuzzy logic systems, neural network (NN), and multi-dimensional Taylor network (MTN), with the traditional backstepping method has become an important research topic and is widely used in general nonlinear systems,[3–5] nonlinear systems with unmodeled dynamics,[6] uncertain nonlinear systems,[7–10] nonlinear systems with input delay,[11] and multiple-input multiple-output (MIMO) nonlinear systems,[12–14] nonlinear time-delay systems,[15] stochastic nonlinear systems with time-varying delays.[16,17] Specifically, the important point is that although a number of advanced MTN-based control methods have been developed for the nonlinear systems, those method is not effective for time-varying delay nonlinear systems subject to input saturation.

In fact, there are many unstable factors in nonlinear systems, such as dead zones, unknown hysteresis and time-delay. The occurrence of these phenomena will lead to the deterioration of system performance and even instability. Therefore, the existence of time-delay cannot be ignored in the design process of control strategy. At present, many meaningful results have been obtained for different types of systems with time-delay, such as nonlinear time-delay systems with dead-zone input,[18,19] nonlinear time-delay systems with full-state constraints,[20,21] and nonlinear uncertain time-delay systems.[22] In existing studies, generalized functions were often used to eliminate the negative effects of unknown time-delay, among which the Lyapunov-Razumikhin function and Lyapunov-Krasovskii function are two effective tools for analyzing and controlling time-delay

[1]School of Mathematics and Physics, Qingdao University of Science and Technology, Qingdao, China
[2]The Research Institute for Mathematics and Interdisciplinary Sciences, Qingdao University of Science and Technology, Qingdao, China

Corresponding author:
Yu-Qun Han, School of Mathematics and Physics, Qingdao University of Science and Technology, No.99 Songling Rd, Qingdao 266061, China.
Email: yuqunhan@163.com

systems. Compared with the former, the latter contains more information about the systematic time delays. Therefore, many interesting results have been reported by constructing Lyapunov-Krasovskii functions. Li et al.,[23] Wang et al.,[24] and Liu et al.[25] used the Lyapunov-Krasovskii function to compensate for the uncertainty of the unknown time-delay. However, the above control approaches did not consider the existence of input constraints.

Actually, due to physical and mechanical manufacturing limitations, controllers often have constraints. Input saturation, an important component of constraints, can disrupt system performance and cause instability. Currently, the methods for dealing with the input saturation can be mainly divided into two types: the compensation method[26–28] and the approximation method.[29,30] Compared with the former, the latter uses a smooth function to directly approximate the nonlinearity, which simplifies the design of the controller and reduces the computational burden. Afterward, this idea was widely applied.[31,32] More recently, MTN-based control method has been applied to nonlinear systems with input saturation.[33,34] However, the above researches did not apply to time-delay nonlinear systems with input saturation constraints, which prompted us to investigate them further.

Based on the above discussion, this paper attempts to provide a new control method for nonlinear systems containing input saturation and time-varying delay, and to achieve a closed-loop system in which all signals are bounded and the tracking error converges to a small neighborhood of the origin. Compared with the existing research results, the main contributions of this paper can be summarized as follows:

(i) The MTN control method is extended to the tracking control problem of nonlinear systems with input saturation and time-varying delay. The proposed scheme based on MTN has the advantages of simple structure, low computational complexity, and good real-time performance. Although MTN control method have been obtained many results,[33,35–40] the literature[33,35–37] did not consider the effect of time-delay terms and the literature[38–40] did not consider input saturation constraints.
(ii) A smooth Gaussian error function is introduced to approximate the saturation signal, and the complex non-smooth input saturation model is transformed into a simple linear model with bounded errors, which simplifies the design process of the controller. The Lyapunov-Krasovskii function is constructed to overcome the adverse effects caused by time-varying delay. Meanwhile, using MTN to approximate the unknown nonlinearity of the systems, an adaptive control strategy is constructed based on the backstepping method.
(iii) Compared with Qian et al.[41] and Li et al.,[42] this paper considers the effect of the input saturation on the system performance, compared with Li and Hong,[43] the time-delay considered in this paper is variable and the research problem is more representative, which relaxes the requirements of existing nonlinear systems with constant time-delay for the time-delay term, and expands the application scope of systems with time-delay.

Problem formulation and preliminaries

Problem description

In this paper, the following nonlinear system is considered

$$\begin{cases} \dot{x}_i = g_i(\bar{\boldsymbol{x}}_i)x_{i+1} + f_i(\bar{\boldsymbol{x}}_i) + h_i(\bar{\boldsymbol{x}}(t-\tau_i(t))) \\ i = 1, \ldots, n-1 \\ \dot{x}_n = g_n(\bar{\boldsymbol{x}}_n)u(v) + f_n(\bar{\boldsymbol{x}}_n) + h_n(\bar{\boldsymbol{x}}(t-\tau_n(t))) \\ y = x_1 \end{cases} \tag{1}$$

where $x_1, x_2, \ldots, x_n$ are the state variables of the control system, $\bar{\boldsymbol{x}}_i = [x_1, x_2, \ldots, x_i]^{\mathrm{T}} \in \boldsymbol{R}^i$ are state vectors, $\bar{\boldsymbol{x}}(t-\tau_i(t)) = [x(t-\tau_1(t)), \ldots, x(t-\tau_i(t))]^{\mathrm{T}} \in \boldsymbol{R}^i$ with $\tau_i(t)$ represents unknown time-varying delays of the state, $h_i(\bar{\boldsymbol{x}}(t-\tau_i(t)))$ are the unknown smooth functions of time-varying delayed states. $y \in \boldsymbol{R}$ indicates the system output. $f_i(\cdot)$ and $g_i(\cdot)$ are the unknown smooth nonlinear functions with $f_i(\mathbf{0}) = 0 (1 \leq i \leq n)$. $u(v): \boldsymbol{R} \to \boldsymbol{R}$ represents the system input with saturated nonlinearity, and its mathematical expression is described as

$$u(v) = \begin{cases} u_M, v > u_M \\ v, u_m \leq v \leq u_M \\ u_m, v < u_m \end{cases} \tag{2}$$

with v, u_m, and u_M are the input, lower bound and upper bound of actuator, respectively. To simplify the notations, the abbreviations $g_i = g_i(\bar{\boldsymbol{x}}_i)$, $f_i = f_i(\bar{\boldsymbol{x}}_i)$, $\tau_i = \tau_i(t)$ are used.

For a given continuous reference signal y_d, the control objective of this article is to design a MTN-based controller and to achieve the following targets: (i) all the signals in the closed-loop systems are bounded; (ii) the tracking error signal $y - y_d$ eventually converges in a small neighborhood near the origin.

The following Assumptions and Lemmas are essential in the controller design process.

Assumption 1[44]: For $\forall i = 1, 2, \cdots, n$, the sign of $g_i(\bar{\boldsymbol{x}}_i)$ is unchanged and there exist constants b_m and b_M such that for $1 \leq i \leq n$, the following inequality is satisfied

$$0 < b_m \leq |g_i(\bar{\boldsymbol{x}}_i)| \leq b_M < \infty, \forall \bar{x}_i \in \boldsymbol{R}^i \tag{3}$$

Remark 1: Assumption 1 indicates that the unknown smooth function $g_i(\bar{\boldsymbol{x}}_i), i = 1, 2, \ldots, n$ is strictly positive or strictly negative. Without loss of generality, we further assume that $0 < b_m \leq g_i(\bar{\boldsymbol{x}}_i) \leq b_M, \forall \bar{\boldsymbol{x}}_i \in \boldsymbol{R}^i$. Since the constants b_m and b_M are not used during the controller design process, it is not necessary to give their specific values.

Lemma 1[45]: If a continuous function $h(x_1,\ldots,x_n):\boldsymbol{R}^{s_1}\times\ldots\times\boldsymbol{R}^{s_n}\to\boldsymbol{R}$ with $h(0,\ldots,0)=0$, where $x_i\in\boldsymbol{R}^{s_i}(i=1,\ldots,n)$ and $s_i>0$. Existence of smooth functions $q_{ij}(\boldsymbol{x}(t))$ such that $|h_i(\boldsymbol{x}(t))|\leq\sum_{j=1}^{n}|z_j(t)|q_{ij}(\boldsymbol{x}(t))$, where $q_{ij}(\boldsymbol{x}(t))>0$, the state variables are $\boldsymbol{x}(t)=[x_1(t),\ldots,x_n(t)]^{\mathrm{T}}$. The coordinate transformation z_j as $z_1=y-y_d$ and $z_i=x_i-\alpha_{i-1}$ $(i=2,\ldots,n)$.

Remark 2: On the basis of Lemma 1, the time-delay term can be represented as $|h_i(\bar{\boldsymbol{x}}(t-\tau_i(t)))|\leq\sum_{j=1}^{n}|z_j(t-\tau_i(t))|q_{ij}(\bar{\boldsymbol{x}}(t-\tau_i(t)))$. Then, the following inequality can be obtained by Young's inequality

$$z_ih_i(\bar{\boldsymbol{x}}(t-\tau_i))\leq\frac{n^2}{4i}z_i^2+\frac{i}{n}\sum_{j=1}^{n}z_j^2(t-\tau_i)q_{ij}^2(x(t-\tau_i)) \tag{4}$$

Assumption 2[45]: For $1\leq i\leq n$, the inequality is holds

$$0<\tau_i\leq\tau_{\max}\qquad\dot{\tau}_i\leq\bar{\tau}_{\max}<1 \tag{5}$$

where $\tau_{\max}$ and $\bar{\tau}_{\max}$ are known constants.

Lemma 2 (Young's inequality[46]): For $\forall(x,y)\in\boldsymbol{R}^2$, satisfying the inequality

$$xy\leq\frac{\gamma^p}{p}|x|^p+\frac{1}{q\gamma^q}|y|^q \tag{6}$$

where $\gamma>0$, the constants $p>1$, $q>1$ and satisfy $(p-1)(q-1)=1$.

Processing of input saturation constraints

Based on Ma et al.,[47] the input saturation $u(v)$ can be expressed as follows

$$u(v)=\breve{u}G_e(\sqrt{\pi}v/2u_M) \tag{7}$$

where $\breve{u}=\left(u_M-\frac{u_m}{2}\right)sign(v)+\left(u_M+\frac{u_m}{2}\right)$, and $G_e(\cdot):\boldsymbol{R}\to\boldsymbol{R}$ is the Gaussian error function. Furthermore, the saturated nonlinear model can be reduced to a linear model as follows

$$u(v)=cv+\varepsilon(v) \tag{8}$$

where $\varepsilon(v)$ is the error of $u(v)$ and cv, c is a constant.

For the convenience of controller design, the error $\varepsilon(v)$ and the reference signal y_d need to satisfy the following Assumptions.

Assumption 3: For c and $\varepsilon(v)$ in (8), there exist three positive constants $\delta>0$, $c_l>0$ and $c_r>0$, such that $|\varepsilon(v)|\leq\delta$, and $c\in[c_l,c_r]$.

Assumption 4: The reference signal y_d and its ith derivative $y_d^{(i)}(i=1,2,\ldots,n)$ are continuous and bounded.

Multi-dimensional Taylor network

In this paper, the MTNs are used to approximate the unknown smooth nonlinear function. For the MTN, the following Lemma is holds.

Lemma 3[48]: Supposing that $f(\boldsymbol{Z})$ is a continuous nonlinear function defined on a compact set Ω. Then for any $\varepsilon>0$, $f(\boldsymbol{Z})$ can be approximated by a MTN with arbitrary accuracy, the following equality hold

$$f(\boldsymbol{Z})=\boldsymbol{\theta}^{\mathrm{T}}P_{m_n}(\boldsymbol{Z})+\delta(\boldsymbol{Z}) \tag{9}$$

where $\boldsymbol{Z}=[z_1,\ldots,z_n]^{\mathrm{T}}\in\boldsymbol{\Omega}\in\boldsymbol{R}^n$ and $\boldsymbol{\theta}=[\theta_1,\ldots,\theta_l]^{\mathrm{T}}\in\boldsymbol{R}^l$ are the input vector and the weight vector of the MTN, respectively. $P_{m_n}(\boldsymbol{Z})=\left[z_1,\cdots,z_n,z_1^2,z_1z_2,\cdots,z_n^2,\cdots,z_1^m,\cdots,z_n^m\right]^{\mathrm{T}}\in\boldsymbol{R}^l$ denotes the intermediate layer of MTN. $\delta(\boldsymbol{Z})$ is the approximation error and satisfies $|\delta(\boldsymbol{Z})|\leq\varepsilon$. n denotes the input dimension, and m and l denote the highest power and the dimension of the intermediate layer, respectively.

Remark 3: It is of interest to note that the advantages of MTN for control have been introduced in the previous work.[15] Specifically, it can be summarized as follows: (1) MTN is particularly suitable for controlling complex nonlinear systems since it has the advantages of fast learning speed and strong approximation ability strong generalization ability; (2) The middle layer of MTN only contains addition and multiplication operations, thus MTN has a simple network structure, which is easier to achieve real-time control. With the arguments above, it can be concluded that compared with NNs, the MTN-based method is of simple structure and less computation.

Remark 4: It is noteworthy that the structure diagram of MTN has been obtained in the recent work.[11,15,49,50] As stated in Zhang and Yan,[49] the value of l can be determined after the values of n and m are given. Theoretically speaking, MTN can achieve the better approximation performance by increasing the value of m. While in practice, the value of m is usually taken as the highest power of function $f(\boldsymbol{Z})$.

Main results

In this section, an adaptive neural control scheme is constructed by using backstepping method and MTN.

First of all, defining the coordinate transformation as follows

$$\begin{cases} z_1 = y - y_d \\ z_i = x_i - \alpha_{i-1}, i = 2, \cdots, n \end{cases} \tag{10}$$

where α_{i-1} is the virtual control signal, the structure of which will be given later.

For each step of the control design, define W_i as follows

$$W_i = \frac{1}{b_m} N_i \|\boldsymbol{\theta}_i\|_2^2, i = 1, \cdots, n \tag{11}$$

where N_i and $\boldsymbol{\theta}_i$ are the number of neurons in the $i-$ th hidden layer and the weight vector, respectively. b_m represents the lower bound of the unknown control direction $g_i(\bar{\boldsymbol{x}}_i)$. In addition, utilizing adaptive parameter $\hat{W}_i$ to estimate W_i, the estimation error is $\tilde{W}_i = W_i - \hat{W}_i$.

Adaptive MTN control design

Step 1: When $i = 1$, according to (1) and (10), the derivative of z_1 is derived as

$$\dot{z}_1 = \dot{x}_1 - \dot{y}_d = g_1 x_2 + f_1 + h_1(\bar{\boldsymbol{x}}(t-\tau_1)) - \dot{y}_d \tag{12}$$

Constructing the Lyapunov-Krasovskii function V_1 as follows

$$V_1 = \frac{1}{2} z_1^2 + \frac{b_m}{2r_1} \tilde{W}_1^2 + \frac{1}{1-\bar{\tau}_{\max}} V_A \tag{13}$$

where $V_A = \sum_{i=1}^{n} \sum_{j=1}^{n} e^{-\kappa(t-\tau_i)} \int_{t-\tau_i}^{t} e^{\kappa s} z_j^2(s) q_{ij}^2(x(s)) ds$. b_m is a constant defined in Assumption 1, $\tilde{W}_1 = W_1 - \hat{W}_1$.

Taking into account (12), by calculating the time derivative of V_1 with respect to time t, one has

$$\begin{aligned} \dot{V}_1 = & z_1(g_1 x_2 + f_1 + h_1(\bar{\boldsymbol{x}}(t-\tau_1)) - \dot{y}_d) \\ & - \frac{b_m}{r_1} \tilde{W}_1 \dot{\hat{W}}_1 + \sum_{i=1}^{n} \sum_{j=1}^{n} \frac{1}{1-\bar{\tau}_{\max}} e^{\kappa \tau_i} z_j^2(t) q_{ij}^2(x(t)) \\ & - \sum_{i=1}^{n} \sum_{j=1}^{n} \frac{\kappa(1-\dot{\tau}_i)}{1-\bar{\tau}_{\max}} e^{-\kappa(t-\tau_i)} \int_{t-\tau_i}^{t} e^{\kappa s} z_j^2(s) q_{ij}^2(x(s)) ds \\ & - \sum_{i=1}^{n} \sum_{j=1}^{n} \frac{(1-\dot{\tau}_i)}{1-\bar{\tau}_{\max}} z_j^2(t-\tau_i) q_{ij}^2(x(t-\tau_i)) \end{aligned} \tag{14}$$

Using Assumption 2, one has $-\kappa(1-\dot{\tau}_i) \leqslant -\kappa(1-\bar{\tau}_{\max})$, that is

$$-\frac{(1-\dot{\tau}_i)}{1-\bar{\tau}_{\max}} \leqslant -1 \tag{15}$$

Reordering the summation terms in (14) yields

$$\sum_{i=1}^{n} \sum_{j=1}^{n} e^{\kappa \tau_i} z_j^2(t) q_{ij}^2(x(t)) = \sum_{j=1}^{n} \sum_{i=1}^{n} e^{\kappa \tau_i} z_j^2(t) q_{ij}^2(x(t)) \tag{16}$$

According to (4), we have

$$\begin{aligned} z_1 h_1(\bar{\boldsymbol{x}}(t-\tau_1)) \leqslant & \frac{n^2}{4} z_1^2 \\ & + \frac{1}{n} \sum_{j=1}^{n} z_j^2(t-\tau_1) q_{1j}^2(x(t-\tau_1)) \end{aligned} \tag{17}$$

Combining (14), (15), (16), and (17), one obtains

$$\begin{aligned} \dot{V}_1 \leqslant & z_1(g_1 x_2 + \sigma_1) - \frac{b_m}{r_1} \tilde{W}_1 \dot{\hat{W}}_1 \\ & - \frac{n-1}{n} \sum_{j=1}^{n} z_j^2(t-\tau_1) q_{1j}^2(x(t-\tau_1)) \\ & - \sum_{i=2}^{n} \sum_{j=1}^{n} z_j^2(t-\tau_i) q_{ij}^2(x(t-\tau_i)) - \kappa V_A \\ & + \frac{1}{1-\bar{\tau}_{\max}} \sum_{j=2}^{n} \sum_{i=1}^{n} e^{\kappa \tau_i} z_j^2(t) q_{ij}^2(x(t)) - \frac{1}{2} z_1^2 \end{aligned} \tag{18}$$

where $\sigma_1 = f_1 - \dot{y}_d + \frac{1}{1-\bar{\tau}_{\max}} \sum_{i=1}^{n} z_1 e^{\kappa \tau_{\max}} q_{i1}^2(x(t)) + \frac{n^2}{4} z_1 + \frac{1}{2} z_1$.

By Lemma 3, a MTN with the structure of $\boldsymbol{\theta}_1^{\mathrm{T}} P_{m_1}(\boldsymbol{Z}_1)$ is used to estimate σ_1. In other words, for $\forall \varepsilon_1 > 0$, we have

$$\sigma_1 = \boldsymbol{\theta}_1^{\mathrm{T}} P_{m_1}(\boldsymbol{Z}_1) + \delta_1(\boldsymbol{Z}_1) \tag{19}$$

where $\boldsymbol{Z}_1 = [z_1]^{\mathrm{T}}$, $\boldsymbol{\theta}_1$ and $P_{m_1}(\boldsymbol{Z}_1)$ are the input weight vector, weight vector and intermediate input layer of MTN, respectively. $\delta_1(\boldsymbol{Z}_1)$ is the estimation error and satisfies $|\delta_1(\boldsymbol{Z}_1)| \leqslant \varepsilon_1$.

Combining the condition $P_{m_1}^{\mathrm{T}} P_{m_1} \leqslant N_1$, N_1 is the dimension of P_{m_1} and according to the definition of W_i, we have

$$\begin{aligned} z_1 \sigma_1 \leqslant & \frac{1}{2} a_1^2 + \frac{1}{2a_1^2} z_1^2 \boldsymbol{\theta}_1^{\mathrm{T}} \boldsymbol{\theta}_1 P_{m_1}^{\mathrm{T}} P_{m_1} + \frac{1}{2} z_1^2 + \frac{1}{2} \delta_1^2 \\ \leqslant & \frac{1}{2} a_1^2 + \frac{b_m}{2a_1^2} z_1^2 W_1 + \frac{1}{2} z_1^2 + \frac{1}{2} \varepsilon_1^2 \end{aligned} \tag{20}$$

Combining (20), $\tilde{W}_i = W_i - \hat{W}_i$ and $x_2 = z_2 + \alpha_1$, the (18) can be rewritten as

$$\begin{aligned}\dot{V}_1 \leqslant\ & z_1(g_1 z_2 + g_1\alpha_1) + \frac{1}{2}\left(a_1^2 + \varepsilon_1^2\right) \\ &+ \frac{1}{1-\bar{\tau}_{\max}}\sum_{j=2}^{n}\sum_{i=1}^{n} e^{\kappa\tau_i} z_j^2(t) q_{ij}^2(x(t)) \\ &- \frac{n-1}{n}\sum_{j=1}^{n} z_j^2(t-\tau_1) q_{1j}^2(x(t-\tau_1)) \\ &- \sum_{i=2}^{n}\sum_{j=1}^{n} z_j^2(t-\tau_i) q_{ij}^2(x(t-\tau_i)) - \kappa V_A \\ &+ \frac{b_m}{r_1}\tilde{W}_1\left(\frac{r_1}{2a_1^2}z_1^2 - \dot{\hat{W}}_1\right) + \frac{b_m}{2a_1^2}z_1^2\hat{W}_1\end{aligned} \tag{21}$$

Applying Young's inequality, the following inequality is holds

$$z_1 g_1 z_2 \leqslant \frac{1}{2} g_1 z_1^2 + \frac{1}{2} g_1 z_2^2 \tag{22}$$

Constructing the first virtual control signal α_1 as follows

$$\alpha_1 = -K_1 z_1 - \frac{1}{2a_1^2} z_1 \hat{W}_1 \tag{23}$$

where $K_1 > 0$ is a design constant.

Substituting (22) and (23) into (21), we have

$$\begin{aligned}\dot{V}_1 \leqslant\ & -C_1 z_1^2 + \frac{b_m}{r_1}\tilde{W}_1\left(\frac{r_1}{2a_1^2}z_1^2 - \dot{\hat{W}}_1\right) \\ &+ \frac{1}{1-\bar{\tau}_{\max}}\sum_{j=2}^{n}\sum_{i=1}^{n} e^{\kappa\tau_i} z_j^2(t) q_{ij}^2(x(t)) \\ &- \frac{n-1}{n}\sum_{j=1}^{n} z_j^2(t-\tau_1) q_{1j}^2(x(t-\tau_1)) \\ &+ \frac{1}{2}\left(a_1^2 + \varepsilon_1^2\right) + \frac{1}{2} g_1 z_2^2 - \kappa V_A \\ &- \sum_{i=2}^{n}\sum_{j=1}^{n} z_j^2(t-\tau_i) q_{ij}^2(x(t-\tau_i))\end{aligned} \tag{24}$$

where $C_1 = \left(K_1 - \frac{1}{2}\right) b_m > 0$ and the term $\frac{1}{2} g_1 z_2^2$ will be dealt with in the next step.

Step $2 \leqslant k \leqslant n-1$: When $i = k$, according to (1) and (10), the derivative of z_k is derived as

$$\dot{z}_k = g_k x_{k+1} + f_k + h_k(\bar{\boldsymbol{x}}(t-\tau_k)) - \dot{\alpha}_{k-1} \tag{25}$$

where $\dot{\alpha}_{k-1} = \sum_{m=1}^{k-1} \frac{\partial\alpha_{k-1}}{\partial x_m}\left(g_m x_{m+1} + f_m + h_m(\bar{\boldsymbol{x}}(t-\tau_m))\right) + \sum_{m=1}^{k-1} \frac{\partial\alpha_{k-1}}{\partial \hat{W}_m}\dot{\hat{W}}_m + \sum_{m=0}^{k-1} \frac{\partial\alpha_{k-1}}{\partial y_d^{(m)}} y_d^{(m+1)}$.

The Lyapunov-Krasovskii function V_k is chosen as

$$V_k = V_{k-1} + \frac{1}{2}z_k^2 + \frac{b_m}{2r_k}\tilde{W}_k^2 \tag{26}$$

Calculating the derivative of V_k with respect to time t, we have

$$\begin{aligned}\dot{V}_k =\ & \dot{V}_{k-1} - \frac{b_m}{r_k}\tilde{W}_k\dot{\hat{W}}_k \\ &+ z_k\left(g_k x_{k+1} + f_k + h_k(\bar{\boldsymbol{x}}(t-\tau_k)) - \dot{\alpha}_{k-1}\right)\end{aligned} \tag{27}$$

Using Lemma 1 and Remark 2, the following inequality can be obtained

$$\begin{aligned} z_k h_k(\bar{\boldsymbol{x}}(t-\tau_k)) \leqslant\ & \frac{n^2}{4k} z_k^2 \\ &+ \frac{k}{n}\sum_{j=1}^{n} z_j^2(t-\tau_k) q_{kj}^2(x(t-\tau_k))\end{aligned} \tag{28}$$

For the complex term $-z_k \sum_{m=1}^{k-1} \frac{\partial\alpha_{k-1}}{\partial x_m} h_m(\bar{\boldsymbol{x}}(t-\tau_m))$ in $\dot{\alpha}_{k-1}$, according to (4), inequality (29) is holds.

$$\begin{aligned} &- z_k \sum_{m=1}^{k-1} \frac{\partial\alpha_{k-1}}{\partial x_m} h_m(\bar{\boldsymbol{x}}(t-\tau_m)) \\ &\leqslant \sum_{m=1}^{k-1} \frac{n^2}{4} z_k^2 \left(\frac{\partial\alpha_{k-1}}{\partial x_m}\right)^2 \\ &+ \frac{1}{n}\sum_{l=1}^{k-1}\sum_{j=1}^{n} z_j^2(t-\tau_l) q_{lj}^2(x(t-\tau_l))\end{aligned} \tag{29}$$

Substituting (28) and (29) into (27) yields

$$\begin{aligned}\dot{V}_k \leqslant\ & \dot{V}_{k-1} + z_k(g_k x_{k+1} + \sigma_k) - \frac{b_m}{r_k}\tilde{W}_k\dot{\hat{W}}_k \\ &- \frac{1}{1-\bar{\tau}_{\max}}\sum_{i=1}^{n} e^{\kappa\tau_{\max}} z_k^2 q_{ik}^2(x(t)) \\ &+ \frac{k}{n}\sum_{j=1}^{n} z_j^2(t-\tau_k) q_{kj}^2(x(t-\tau_k)) - \frac{1}{2}z_k^2 \\ &+ \frac{1}{n}\sum_{j=1}^{n} z_j^2(t-\tau_l) q_{lj}^2(x(t-\tau_l)) - \frac{1}{2}z_k^2 g_{k-1}\end{aligned} \tag{30}$$

where $\sigma_k = f_k + \sum_{m=1}^{k-1} \frac{n^2}{4}\left(\frac{\partial\alpha_{k-1}}{\partial x_m}\right)^2 z_k - \sum_{m=1}^{k-1} \frac{\partial\alpha_{k-1}}{\partial \hat{W}_m}\cdot \dot{\hat{W}}_m - \sum_{m=0}^{k-1} \frac{\partial\alpha_{k-1}}{\partial y_d^{(m)}} y_d^{(m+1)} - \sum_{m=1}^{k-1}\left(\frac{\partial\alpha_{k-1}}{\partial x_m}\right)(f_m + g_m x_{m+1}) + \frac{n^2}{4k} z_k + \frac{1}{2} z_k + \frac{1}{2} g_{k-1} z_k + \frac{1}{1-\bar{\tau}_{\max}} \sum_{i=1}^{n} z_k e^{\kappa\tau_{\max}} q_{ik}^2(x(t))$

Since the nonlinear function σ_k is unknown, according to Lemma 3, MTN is used to approximate σ_k with $\forall \varepsilon_k > 0$, that is

$$\sigma_k = \boldsymbol{\theta}_k^{\mathrm{T}} P_{m_k}(\boldsymbol{Z}_k) + \delta_k(\boldsymbol{Z}_k) \tag{31}$$

where $\boldsymbol{Z}_k = [z_1, \ldots, z_k]^{\mathrm{T}}$, $\boldsymbol{\theta}_k$ and $P_{m_k}(\boldsymbol{Z}_k)$ are the input weight vector, weight vector and intermediate input layer of MTN, respectively. $\delta_k(\boldsymbol{Z}_k)$ is the estimation error and satisfies $|\delta_k(\boldsymbol{Z}_k)| \leqslant \varepsilon_k$.

According to (11), and noting that $P_{m_k}^{\mathrm{T}} P_{m_k} \leqslant N_k$, we have

$$z_k \sigma_k \leqslant \frac{1}{2} a_k^2 + \frac{b_m}{2a_k^2} z_k^2 W_k + \frac{1}{2} z_k^2 + \frac{1}{2} \varepsilon_k^2 \tag{32}$$

Combining (32) and taking $x_{k+1} = z_{k+1} + \alpha_k$, $W_k = \hat{W}_k + \tilde{W}_k$ into account, the inequality (30) can be transformed into the following form

$$\begin{aligned} \dot{V}_k \leqslant\, & z_k(g_k \alpha_k + g_k z_{k+1}) + \frac{1}{2}\sum_{j=1}^{k}\left(a_j^2 + \varepsilon_j^2\right) \\ & - \frac{n-k}{n}\sum_{l=1}^{k}\sum_{j=1}^{n} z_j^2(t-\tau_l) q_{lj}^2(x(t-\tau_l)) \\ & + \frac{1}{1-\bar{\tau}_{\max}}\sum_{j=k+1}^{n}\sum_{i=1}^{n} e^{\kappa\tau_i} z_j^2(t) q_{ij}^2(x(t)) \\ & - \sum_{i=k+1}^{n}\sum_{j=1}^{n} z_j^2(t-\tau_i) q_{ij}^2(x(t-\tau_i)) \\ & - \kappa V_A - \sum_{j=1}^{k-1} C_j z_j^2 + \frac{b_m}{2a_k^2} z_k^2 \hat{W}_k \\ & + \sum_{j=1}^{k} \frac{b_m}{r_j} \tilde{W}_j \left(\frac{r_j}{2a_j^2} z_j^2 - \dot{\hat{W}}_j\right) \end{aligned} \tag{33}$$

Constructing the virtual control variable α_k as

$$\alpha_k = -K_k z_k - \frac{1}{2a_k^2} z_k \hat{W}_k \tag{34}$$

where $K_k > 0$ is the design constant.

Then, using Assumption 1, we have

$$\begin{aligned} z_k g_k \alpha_k &= -g_k K_k z_k^2 - g_k \frac{1}{2a_k^2} z_k^2 \hat{W}_k \\ &\leqslant -K_k g_k z_k^2 - \frac{b_m}{2a_k^2} z_k^2 \hat{W}_k \end{aligned} \tag{35}$$

According to Young's inequality, the following inequality can be obtained

$$z_k g_k z_{k+1} \leqslant \frac{1}{2} g_k z_k^2 + \frac{1}{2} g_k z_{k+1}^2 \tag{36}$$

Substituting (35) and (36) into (33), one has

$$\begin{aligned} \dot{V}_k \leqslant\, & -\sum_{j=1}^{k} C_j z_j^2 + \frac{1}{2} g_k z_{k+1}^2 - \kappa V_A \\ & - \sum_{i=k+1}^{n}\sum_{j=1}^{n} z_j^2(t-\tau_i) q_{ij}^2(x(t-\tau_i)) \\ & - \frac{n-k}{n}\sum_{l=1}^{k}\sum_{j=1}^{n} z_j^2(t-\tau_l) q_{lj}^2(x(t-\tau_l)) \\ & + \frac{1}{1-\bar{\tau}_{\max}}\sum_{j=k+1}^{n}\sum_{i=1}^{n} e^{\kappa\tau_i} z_j^2(t) q_{ij}^2(x(t)) \\ & + \frac{1}{2}\sum_{j=1}^{k}\left(a_j^2 + \varepsilon_j^2\right) + \sum_{j=1}^{k} \frac{b_m}{r_j} \tilde{W}_j \left(\frac{r_j}{2a_j^2} z_j^2 - \dot{\hat{W}}_j\right) \end{aligned} \tag{37}$$

where $C_j = b_m\left(K_j - \frac{1}{2}\right) > 0, (j = 1, \cdots, n-1)$.

Step n: When $i = n$, according to (1) and (10), the derivative of z_n is derived as

$$\dot{z}_n = g_n u + f_n + h_n(\bar{\boldsymbol{x}}(t-\tau_n)) - \dot{\alpha}_{n-1} \tag{38}$$

where $\dot{\alpha}_{n-1} = \sum_{m=1}^{n-1} \frac{\partial \alpha_{n-1}}{\partial \hat{W}_m} \dot{\hat{W}}_m + \sum_{m=0}^{n-1} \frac{\partial \alpha_{n-1}}{\partial y_d^{(m)}} y_d^{(m+1)} + \sum_{m=1}^{n-1} \frac{\partial \alpha_{n-1}}{\partial x_m}(g_m x_{m+1} + f_m + h_m(\bar{\boldsymbol{x}}(t-\tau_m)))$.

Constructing the Lyapunov-Krasovskii function V_n as follows

$$V_n = V_{n-1} + \frac{1}{2} z_n^2 + \frac{b_m}{2r_n} \tilde{W}_n^2 \tag{39}$$

Calculating the derivative of V_n with respect to time t, it produces

$$\begin{aligned} \dot{V}_n = \dot{V}_{n-1} - \frac{b_m}{r_n} \tilde{W}_n \dot{\hat{W}}_n \\ + z_n(g_n u + f_n + h_n(\bar{\boldsymbol{x}}(t-\tau_n)) - \dot{\alpha}_{n-1}) \end{aligned} \tag{40}$$

Using Lemma 1 and Remark 2, the following inequality holds

$$\begin{aligned} & z_n h_n(\bar{\boldsymbol{x}}(t-\tau_n)) \\ & \quad \leqslant \frac{n^2}{4n} z_n^2 + \frac{n}{n}\sum_{j=1}^{n} z_j^2(t-\tau_n) q_{nj}^2(x(t-\tau_n)) \end{aligned} \tag{41}$$

According to (4), dealing with the complex term $-z_n \sum_{m=1}^{n-1} \frac{\partial \alpha_{n-1}}{\partial x_m} h_m(\bar{\boldsymbol{x}}(t-\tau_m))$, the following inequality can be obtained

$$- z_n \sum_{m=1}^{n-1} \frac{\partial \alpha_{n-1}}{\partial x_m} h_m(\bar{\boldsymbol{x}}(t-\tau_m)) \leqslant \sum_{m=1}^{n-1} \frac{n^2}{4} z_n^2 \left(\frac{\partial \alpha_{n-1}}{\partial x_m}\right)^2 + \frac{1}{n}\sum_{l=1}^{n-1}\sum_{j=1}^{n} z_j^2(t-\tau_l) q_{lj}^2(x(t-\tau_l)) \tag{42}$$

Using (41) and (42), (40) can be given in the following form

$$\begin{aligned} \dot{V}_n \leqslant{}& \dot{V}_{n-1} - \frac{b_m}{r_n}\tilde{W}_n\dot{\hat{W}}_n - \frac{1}{2}z_n^2 - \frac{1}{2}g_{n-1}z_n^2 \\ &- \frac{1}{1-\bar{\tau}_{\max}}\sum_{i=1}^{n} e^{\kappa\tau_{\max}} z_n^2 q_{in}^2(x(t)) \\ &+ \sum_{j=1}^{n} z_j^2(t-\tau_n) q_{nj}^2(x(t-\tau_n)) \\ &+ z_n(g_n u + \sigma_n) \\ &+ \frac{1}{n}\sum_{l=1}^{n-1}\sum_{j=1}^{n} z_j^2(t-\tau_l) q_{lj}^2(x(t-\tau_l)) \end{aligned} \tag{43}$$

where $\sigma_n = f_n + \sum_{m=1}^{n-1} \frac{n^2}{4}\left(\frac{\partial\alpha_{n-1}}{\partial x_m}\right)^2 z_n - \sum_{m=1}^{n-1}\frac{\partial\alpha_{n-1}}{\partial\hat{W}_m}\dot{\hat{W}}_m - \cdot \sum_{m=1}^{n-1}\left(\frac{\partial\alpha_{n-1}}{\partial x_m}\right)(f_m + g_m x_{m+1}) - \sum_{m=0}^{n-1}\frac{\partial\alpha_{n-1}}{\partial y_d^{(m)}} y_d^{(m+1)} + \frac{1}{1-\bar{\tau}_{\max}}\sum_{i=1}^{n}|z_n| e^{\kappa\tau_{\max}} q_{in}^2(x(t)) + \left(\frac{n^2}{4n} + \frac{1}{2} + \frac{1}{2}g_{n-1}\right) z_n$

Similarly to step k, the MTN is used to approximate the unknown nonlinear function σ_n, for any accuracy $\varepsilon_n > 0$, that is

$$\sigma_n = \boldsymbol{\theta}_n^{\mathrm{T}} P_{m_n}(\boldsymbol{Z}_n) + \delta_n(\boldsymbol{Z}_n) \tag{44}$$

where $\boldsymbol{Z}_n = [z_1, \ldots, z_n]^{\mathrm{T}}$ and $\boldsymbol{\theta}_n$ are the input weight vector and weight vector, respectively. $\delta_n(\boldsymbol{Z}_n)$ is the estimation error and satisfies $|\delta_n(\boldsymbol{Z}_n)| \leqslant \varepsilon_n$.

Combining the condition $P_{m_n}^{\mathrm{T}} P_{m_n} \leqslant N_n$, we have

$$\begin{aligned} z_n\sigma_n &\leqslant \frac{1}{2}a_n^2 + \frac{1}{2a_n^2} z_n^2 \boldsymbol{\theta}_n^{\mathrm{T}}\boldsymbol{\theta}_n P_{m_n}^{\mathrm{T}} P_{m_n} + \frac{1}{2}z_n^2 + \frac{1}{2}\delta_n^2 \\ &\leqslant \frac{1}{2}a_n^2 + \frac{b_m}{2a_n^2} z_n^2 W_n + \frac{1}{2}z_n^2 + \frac{1}{2}\varepsilon_n^2 \end{aligned} \tag{45}$$

Combining (8), (37) with $k = n-1$ and (45), the following inequality can be obtained

$$\begin{aligned} \dot{V}_n \leqslant{}& z_n g_n(c\boldsymbol{v} + \varepsilon(\boldsymbol{v})) + \frac{b_m}{2a_n^2} z_n^2 \hat{W}_n - \sum_{j=1}^{n-1} C_j z_j^2 \\ &- \kappa V_A + \sum_{j=1}^{n} \frac{b_m}{r_j}\tilde{W}_j\left(\frac{r_j}{2a_j^2}z_j^2 - \dot{\hat{W}}_j\right) \\ &+ \frac{1}{2}\sum_{j=1}^{n}\left(a_j^2 + \varepsilon_j^2\right) \end{aligned} \tag{46}$$

Based on (46), designing the actual control signals $\boldsymbol{v}$ as follows

$$\boldsymbol{v} = -\frac{1}{c_l}\left(K_n|z_n| + \frac{1}{2a_n^2}\hat{W}_n|z_n|\right) sign(z_n) \tag{47}$$

where $K_n > 0$ and $c_l > 0$ are constants, and $c \in [c_l, c_r]$.

Then the term $z_n g_n c\boldsymbol{v}$ can be transformed into

$$z_n g_n c\boldsymbol{v} \leqslant -K_n b_m z_n^2 - \frac{b_m}{2a_n^2}\hat{W}_n z_n^2 \tag{48}$$

According to Assumption 3, we can obtain

$$z_n g_n \varepsilon(\boldsymbol{v}) \leqslant \frac{1}{2} b_M z_n^2 + \frac{1}{2} b_M \delta^2 \tag{49}$$

Then, substituting (47), (48), and (49) into (46), the following inequality holds

$$\begin{aligned} \dot{V}_n \leqslant{}& -\sum_{j=1}^{n} C_j z_j^2 + \frac{1}{2}\sum_{j=1}^{n}\left(a_j^2 + \varepsilon_j^2\right) - \kappa V_A \\ &+ \sum_{j=1}^{n}\frac{b_m}{r_j}\tilde{W}_j\left(\frac{r_j}{2a_j^2}z_j^2 - \dot{\hat{W}}_j\right) + \frac{1}{2}b_M\delta^2 \end{aligned} \tag{50}$$

where $C_j = \begin{cases} b_m\left(K_j - \frac{1}{2}\right) > 0, j = 1, \ldots, n-1 \\ b_m K_n - \frac{1}{2}b_M, j = n \end{cases}$, and $C_j > 0$.

Up to now, we have completed the design process of the control strategy, which is shown in Figure 1.

Stability analysis

In this section, the Lyapunov theory is used to analyze the stability of closed-loop systems.

Theorem 1: Under Assumptions 1–4, considering the closed-loop system consisting of system (1), the virtual control signals (23), (34), and the actual control signal (47), with the adaptive laws defined as follows

$$\dot{\hat{W}}_j = \frac{r_j}{2a_j^2} z_j^2 - p_j\hat{W}_j \tag{51}$$

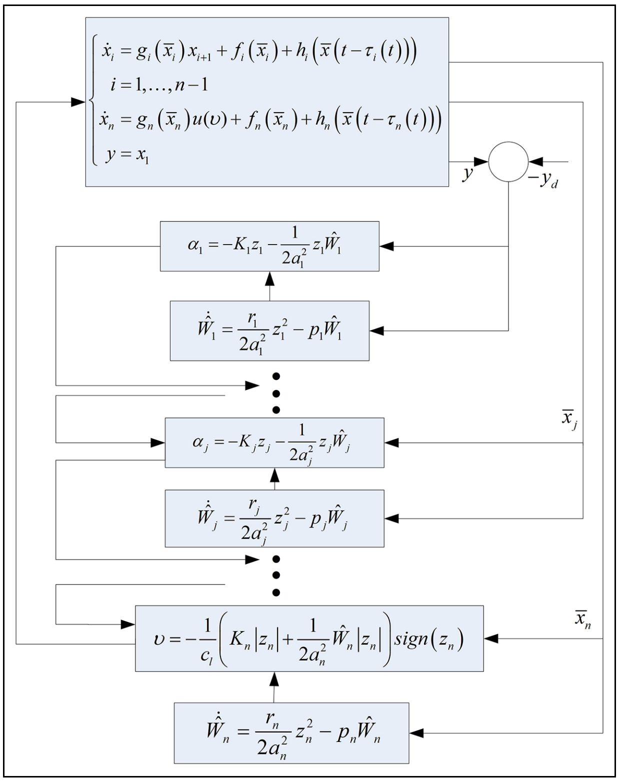

Figure 1. Block diagram of the control design process.

where $j = 1, \ldots, n$ and $p_j > 0$ are design parameters. Then, for any bounded initial condition, all signals in the closed-loop system are bounded, and the error signal eventually converges in a small neighborhood near the origin.

Proof: For the closed-loop system, considering the Lyapunov function V as $V = V_n$.

Then, substituting (51) into $\dot{\hat{W}}_j$, the following inequality holds

$$\sum_{j=1}^{n} \frac{b_m}{r_j} \tilde{W}_j \left(\frac{r_j}{2a_j^2} z_j^2 - \dot{\hat{W}}_j \right) \leq \sum_{j=1}^{n} \frac{b_m}{2r_j} p_j W_j^2 - \sum_{j=1}^{n} \frac{b_m}{2r_j} p_j \tilde{W}_j^2 \tag{52}$$

Substitute (52) into (50), one has

$$\dot{V} \leq -\sum_{j=1}^{n} C_j z_j^2 - \sum_{j=1}^{n} \frac{b_m}{2r_j} p_j \tilde{W}_j^2 + \frac{1}{2} b_M \delta^2 + \frac{1}{2} \sum_{j=1}^{n} \left(a_j^2 + \varepsilon_j^2 \right) + \sum_{j=1}^{n} \frac{b_m}{2r_j} p_j W_j^2 - \kappa V_A \tag{53}$$

Here, let $a_0 = \min\{2C_j, p_j, \kappa(1 - \bar{\tau}_{\max}), j = 1, \cdots, n\}$ and $b_0 = \frac{1}{2}\sum_{j=1}^{n}(a_j^2 + \varepsilon_j^2) + \sum_{j=1}^{n} \frac{b_m}{2r_j} p_j W_j^2 + \frac{1}{2} b_M \delta^2$.

Then, (53) can be rewritten in the following form

$$\dot{V} \leq -a_0 V_n + b_0 \tag{54}$$

From (54), the following inequality is given

$$V \leq \left(V_n(0) - \frac{b_0}{a_0} \right) e^{-a_0 t} + \frac{b_0}{a_0} \tag{55}$$

Inequality (55) means that V_n is bounded by $\frac{b_0}{a_0}$. Therefore, recalling the definition of V, we can see that all signals in the closed-loop system are bounded.

In addition, when $t \to \infty$, it follows that

$$z_1^2 = (y - y_d)^2 \leq \frac{2b_0}{a_0} \tag{56}$$

The above inequality means that the tracking error $y - y_d$ converges to a small neighborhood near the origin by properly adjusting a_0 and b_0.

Therefore, the proof of Theorem 1 is completed.

Remark 5: There are many design parameters involved in the design process. Following the design and analysis above, the tracking effect can be improved by increasing a_0 or decreasing b_0. Therefore, we can increase a_0 by increasing C_j and p_j, and decrease b_0 by decreasing p_j, ε_j, and δ, etc. However, b_0 also enlarges when increasing p_j, which in turn affects the tracking effect, and the value of u is also affected when K_j is too large. Consequently, in practical application, the parameters should be select carefully for the sake of achieving better results.

Simulation

In this section, three simulation examples are used to illustrate the effectiveness of the proposed control method.

Example 1 (Numerical example): Considering the following third-order nonlinear system containing input saturation and time-varying delay

$$\begin{cases} \dot{x}_1 = x_2 - 0.2x_1 e^{x_1} + h_1(\bar{\boldsymbol{x}}(t - \tau_1(t))) \\ \dot{x}_2 = x_3 + x_1 \sin x_2 + h_2(\bar{\boldsymbol{x}}(t - \tau_2(t))) \\ \dot{x}_3 = u + x_1 x_2 x_3 + h_3(\bar{\boldsymbol{x}}(t - \tau_3(t))) \\ y = x_1 \end{cases} \tag{57}$$

with the initial states are chosen as $[x_1(0), x_2(0), x_3(0)]^T = [0, 0, 0]^T$ and given the reference signal $y_d = 0.1 \sin t$. The time-delayed terms are selected as $h_1(\bar{\boldsymbol{x}}(t - \tau_1(t))) = 0.05 \sin(x_1(t - \tau_1(t)))$, $h_2(\bar{\boldsymbol{x}}(t - \tau_2(t))) = 0.01 x_1(t - \tau_1(t)) x_2(t - \tau_2(t))$ and $h_3(\bar{\boldsymbol{x}}(t - \tau_3(t))) = 0.01 \cos(x_3(t - \tau_3(t)))$.

In simulation, the time delays are chosen as $\tau_1(t) = 0.02 + 0.01 \sin(0.1t)$, $\tau_2(t) = 0.05 + 0.2 \sin t$

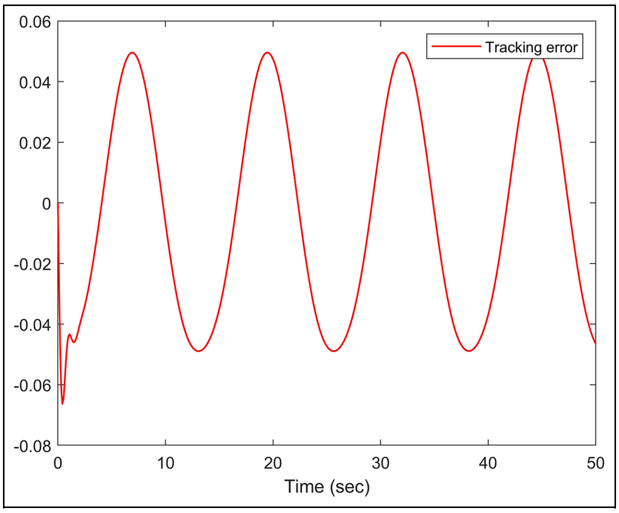

Figure 2. The curve of tracking error of system (57).

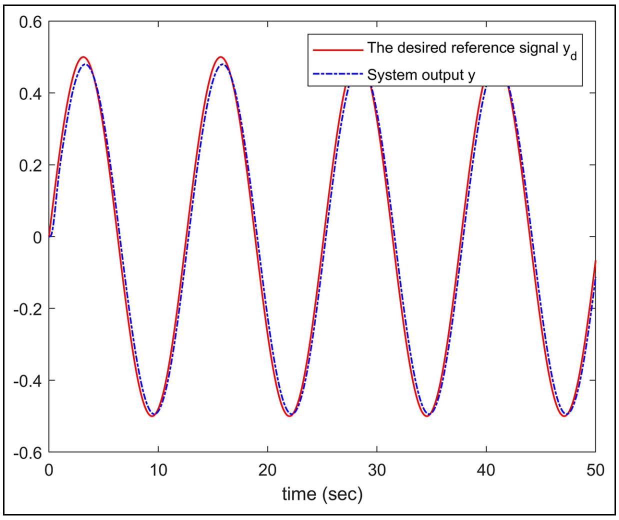

Figure 3. The variation curves of y and y_d of system (57).

and $\tau_3(t) = 0.05 + 0.3\sin t$. The saturation parameters are selected as $u_M = 4$ and $u_m = -4$. The positive parameters are chosen as $p_1 = 5$, $p_2 = 0.1$, $p_3 = 10$, $K_1 = 5.2$, $K_2 = 5$, $K_3 = 50$, $d = 5$, $a_1 = 5$, $a_2 = 10$, $a_3 = 1$, $r_1 = 1$, $r_2 = 1$, and $r_3 = 2$, respectively.

The simulation results are shown in Figures 2 to 5, respectively. Figure 2 shows the results for the tracking error $y - y_d$, which indicates that the tracking error converges to a small neighborhood near the origin. Figure 3 shows the trajectory curves of the actual output y and the reference signal y_d. Figure 4 gives the responses of control signals u and v. Figure 5 shows the variation curves of the state variables x_2 and x_3, indicating that all signals in the closed-loop system are bounded. Therefore, the controller designed in this paper is effective.

Example 2 (Practical example): For the sake of further verifying the effectiveness of the proposed method, a class of single-link manipulator containing actuator

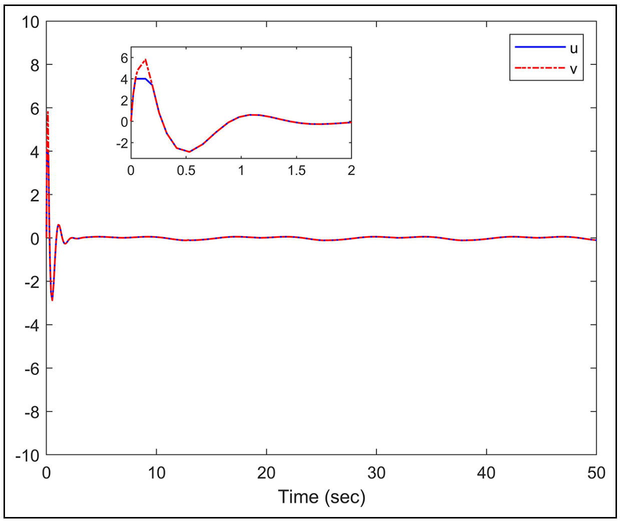

Figure 4. The responses of u and v of system (57).

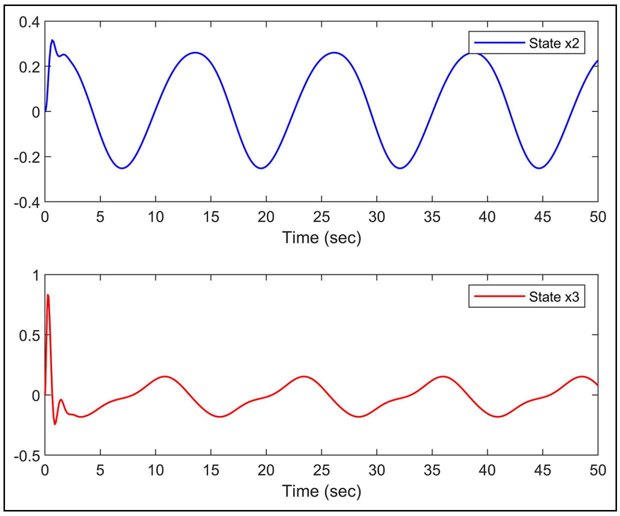

Figure 5. State variables x_2 and x_3 of system (57).

dynamics system is considered. According to Liu et al.,[51] its dynamics system can be described as follows

$$\begin{cases} \dot{x}_1 = x_2 + h_1(\bar{\mathbf{x}}(t-\tau_1(t))) \\ \dot{x}_2 = \frac{1}{M}x_3 - \frac{N}{M}\sin x_1 - \frac{B}{M}x_2 + h_2(\bar{\mathbf{x}}(t-\tau_2(t))) \\ \dot{x}_3 = \frac{1}{D}u - \frac{K_m}{D}x_2 - \frac{H}{D}x_3 + h_3(\bar{\mathbf{x}}(t-\tau_3(t))) \\ y = x_1 \end{cases} \tag{58}$$

where $h_1(\bar{\mathbf{x}}(t-\tau_1(t))) = 0.05\sin(x_1(t-\tau_1(t)))$, $h_2(\bar{\mathbf{x}}(t-\tau_2(t))) = 0.01x_1(t-\tau_1(t))x_2(t-\tau_2(t))$ and $h_3(\bar{\mathbf{x}}(t-\tau_3(t))) = 0.01\cos(x_3(t-\tau_3(t)))$ are time-delayed terms. The parameters of (58), such as M, N,B, D, H, and K_m, are the same as in Liu et al.[51] The initial states are chosen as $x_1(0) = x_2(0) = x_3(0) = 0$, the reference signal is chosen as $y_d = 0.1\sin t$, and the time delays are chosen as $\tau_1(t) = 0.01\sin t$, $\tau_2(t) = 0.05 + 0.1\sin t$, and $\tau_3(t) = 0.1\sin(0.5t)$, respectively.

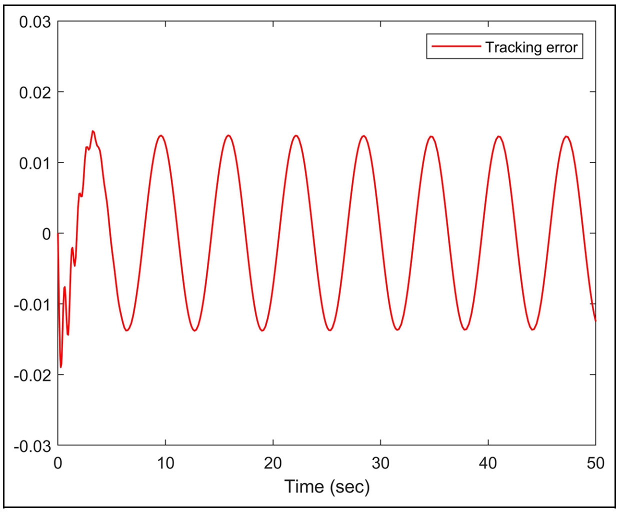

Figure 6. The curve of tracking error of system (58).

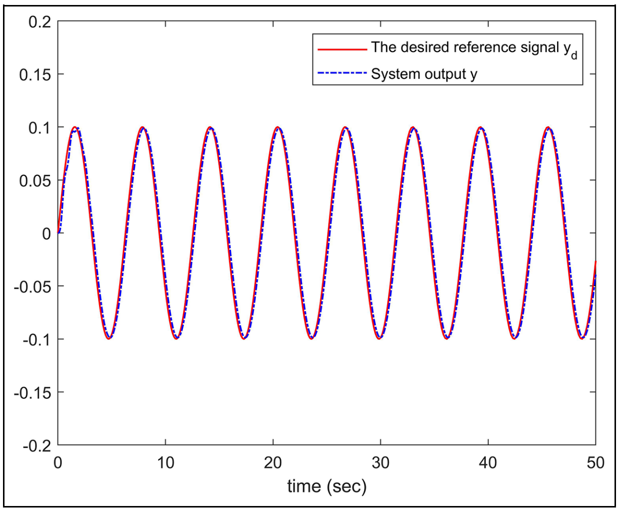

Figure 7. The variation curves of y and y_d of system (58).

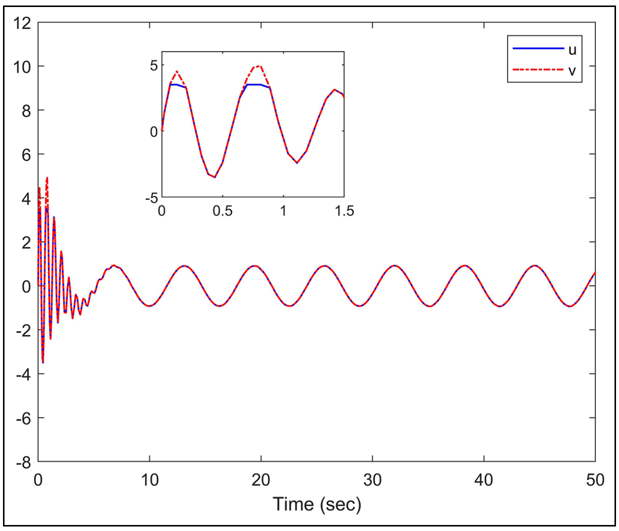

Figure 8. The responses of u and v of system (58).

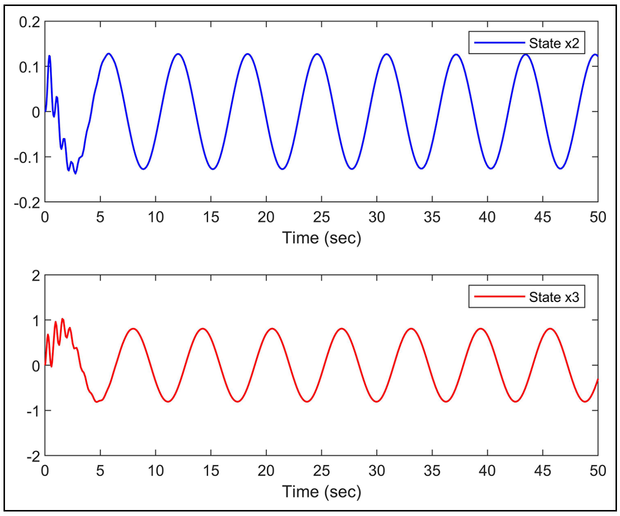

Figure 9. State variables x_2 and x_3 of system (58).

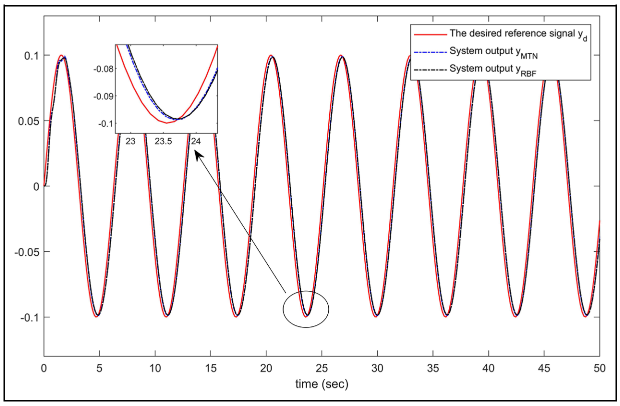

Figure 10. Trajectory comparison results of MTN and RBF.

In simulation, the saturated nonlinear parameters are selected as $u_m = -3.5$ and $u_M = 3.5$. The parameters of the control structure are selected as $K_1 = 8$, $K_2 = 10$, $K_3 = 45$, respectively.

The simulation results of system (58) are shown in the Figures 6 to 9. Figure 6 reveals that the tracking error of the system (58). Figure 7 shows the trajectories of output y and the reference signal y_d. Figure 8 displays the responses of control signal u and v. Figure 9 shows the responses of system states x_2 and x_3. Thus, as can be seen in Figures 7 to 9, all signals in the closed loop are bounded.

The results further indicate that the control method proposed in this paper is effective and still achieves satisfactory results for practical systems.

Example 3 (Comparative example): In order to further illustrate the advantages of the proposed control method, for system (58), a comparative example is conducted on the MTN and radial basis function (RBF) NN methods. The concrete practice is to replace MTNs with RBF NNs in the control scheme. The comparison results are displayed in Figure 10.

From Figure 10, it can be seen that both of the above two methods can achieve tracking control. Considering the MTN has the advantage of low computational complexity, we can conclude that the control scheme proposed in this paper can achieve satisfactory control results at a small calculate costs.

Conclusion

The MTN-based adaptive control algorithm is proposed for a class of nonlinear systems with input saturation and time-varying delay. In the controller design process, the unknown nonlinearity of the system is approximated by using MTN, the Gaussian error function is introduced to overcome the effect of input saturation, and the Lyapunov-Krasovskii function is used to deal with the unknown time-delay, which compensates the negative effect caused by time-varying delay. Then, a control scheme is proposed based on the adaptive backstepping technique and Lyapunov stability theory. The results show that the proposed method can ensure that all signals of the closed-loop system are bounded and achieve convergence of the tracking error to a small neighborhood near the origin. Finally, the effectiveness of the method is verified by simulations. For the purpose of application, our future work will devote to extend the proposed approach to time-varying delayed nonlinear systems subject to state constraints and input saturation.

Declaration of conflicting interests

The author(s) declared no potential conflicts of interest with respect to the research, authorship, and/or publication of this article.

Funding

The author(s) disclosed receipt of the following financial support for the research, authorship, and/or publication of this article: This work was supported by the Shandong Provincial Natural Science Foundation, China (No. ZR2020QF055).

ORCID iD

Yu-Qun Han https://orcid.org/0000-0002-9055-2954

Data availability statement

Data sharing is not applicable to this article as no new data were created or analyzed in this study.

References

1. Zhao X, Zheng X, Niu B, et al. Adaptive tracking control for a class of uncertain switched nonlinear systems. *Automatica* 2015; 52: 185–191.
2. Rehan M, Hong KS and Ge SS. Stabilization and tracking control for a class of nonlinear systems. *Nonlinear Anal Real World Appl* 2011; 12(3): 1786–1796.
3. Chen M, Wang H and Liu X. Adaptive fuzzy practical fixed-time tracking control of nonlinear systems. *IEEE Trans Fuzzy Syst* 2021; 29(3): 664–673.
4. Feng Z, Li RB and Zheng WX. Event-based adaptive neural network asymptotic tracking control for a class of nonlinear systems. *Inf Sci* 2022; 612: 481–495.
5. Li K and Li Y. Adaptive neural network finite-time dynamic surface control for nonlinear systems. *IEEE Trans Neural Netw Learn Syst* 2021; 32(12): 5688–5697.
6. Xu K, Wang H and Liu PX. Adaptive fuzzy finite-time tracking control of nonlinear systems with unmodeled dynamics. *Appl Math Comput* 2023; 450: 127992.
7. Chen W, Wang J, Ma K, et al. Novel adaptive neural networks control with event-triggered for uncertain nonlinear system. *J Franklin Inst* 2020; 357(15): 10410–10431.
8. Deng X, Zhang C and Ge Y. Adaptive neural network dynamic surface control of uncertain strict-feedback nonlinear systems with unknown control direction and unknown actuator fault. *J Franklin Inst* 2022; 359(9): 4054–4073.
9. Su H, Zhang T and Zhang W. Fuzzy adaptive control for SISO nonlinear uncertain systems based on backstepping and small-gain approach. *Neurocomputing* 2017; 238: 212–226.
10. Yan H and Kang A. Asymptotic tracking and dynamic regulation of SISO non-linear system based on discrete multi-dimensional Taylor network. *IET Control Theory Appl* 2017; 11(10): 1619–1626.
11. Wang GB, Yan HS and Zheng XY. Contraction-based stochastic model predictive control for nonlinear systems with input delay using multi-dimensional Taylor network. *IEEE Trans Automat Contr* 2023; 68(12): 7498–7513.
12. Zhou Y and Wang X. Adaptive fuzzy command filtering control for nonlinear MIMO systems with full state constraints and unknown control direction. *Neurocomputing* 2022; 493: 474–485.
13. Shi W. Adaptive fuzzy output-feedback control for nonaffine MIMO nonlinear systems with prescribed performance. *IEEE Trans Fuzzy Syst* 2021; 29(5): 1107–1120.
14. Wang S, Xia J, Sun W, et al. Observer-based adaptive event-triggered tracking control for nonlinear MIMO systems based on neural networks technique. *Neurocomputing* 2021; 433: 71–82.
15. Yan HS and Duan ZY. Tube-based model predictive control using multidimensional Taylor network for nonlinear time-delay systems. *IEEE Trans Automat Contr* 2021; 66(5): 2099–2114.
16. Yan HS and Wang GB. Adaptive tracking control for stochastic nonlinear systems with time-varying delays using multi-dimensional Taylor network. *ISA Trans* 2023; 132: 246–257.
17. Yan H and Wang G. Adaptive control for stochastic nonlinear systems with time-varying delays via multidimensional Taylor network. *Int J Robust Nonlinear Control* 2023; 33(14): 8376–8399.
18. Zhang Z, Park JH, Zhang K, et al. Adaptive control for a class of nonlinear time-delay systems with dead-zone input. *J Franklin Inst* 2016; 353(17): 4400–4421.

19. Yue HY and Li JM. Adaptive fuzzy dynamic surface control for a class of perturbed nonlinear time-varying delay systems with unknown dead-zone. *Int J Autom Comput* 2012; 9(5): 545–554.
20. Li DP and Li DJ. Adaptive neural tracking control for nonlinear time-delay systems with full state constraints. *IEEE Trans Syst Man Cybern Syst* 2017; 47(7): 1590–1601.
21. Wu Y, Xu T and Mo H. Adaptive tracking control for nonlinear time-delay systems with time varying full state constraints. *Trans Inst Meas Contr* 2020; 42(12): 2178–2190.
22. Ning PJ, Hua CC, Li K, et al. A novel theorem for prescribed-time control of nonlinear uncertain time-delay systems. *Automatica* 2023; 152: 111009.
23. Li M, Li S, Ahn CK, et al. Adaptive fuzzy event-triggered command-filtered control for nonlinear time-delay systems. *IEEE Trans Fuzzy Syst* 2022; 30(4): 1025–1035.
24. Wang H, Sun W and Liu PX. Adaptive intelligent control of nonaffine nonlinear time-delay systems with dynamic uncertainties. *IEEE Trans Syst Man Cybern Syst* 2017; 47(7): 1474–1485.
25. Liu Y, Zhu Q and Wang L. Event-based adaptive fuzzy control design for nonstrict-feedback nonlinear time-delay systems with state constraints. *ISA Trans* 2022; 125: 134–145.
26. Hua C, Meng R, Li K, et al. Full state constraints-based adaptive tracking control for uncertain nonlinear stochastic systems with input saturation. *J Franklin Inst* 2020; 357(9): 5125–5142.
27. Song Z, Li P, Wang Z, et al. Adaptive tracking control for switched uncertain nonlinear systems with input saturation and unmodeled dynamics. *IEEE Trans Circuits Syst II Express Briefs* 2020; 67(12): 3152–3156.
28. Wang L and Chen CLP. Reduced-order observer based dynamic event-triggered adaptive NN control for stochastic nonlinear systems subject to unknown input saturation. *IEEE Trans Neural Netw Learn Syst* 2021; 32(4): 1678–1690.
29. Homayoun B, Arefi MM and Vafamand N. Robust adaptive backstepping tracking control of stochastic nonlinear systems with unknown input saturation: a command filter approach. *Int J Robust Nonlinear Control* 2020; 30(8): 3296–3313.
30. Li YD and Chen B. Adaptive neural tracking control for a class of nonlinear systems with input delay and saturation. *Syst Sci Control Eng* 2021; 9: 21–28.
31. Ma L, Zong G, Zhao X, et al. Observed-based adaptive finite-time tracking control for a class of nonstrict-feedback nonlinear systems with input saturation. *J Franklin Inst* 2020; 357(16): 11518–11544.
32. Gao L, Song Z and Wang Z. Adaptive tracking control of uncertain constrained nonlinear systems with input saturation. *Commun Nonlinear Sci Numer Simul* 2023; 127: 107553.
33. Han Y. Adaptive tracking control for a class of stochastic non-linear systems with input saturation constraint using multi-dimensional Taylor network. *IET Control Theory Appl* 2020; 14(9): 1193–1199.
34. Li N, Du Y, Wang D, et al. Adaptive decentralized prescribed performance control for a class of large-scale stochastic nonlinear systems subject to input saturation and full state constraints. *Int J Adapt Control Signal Process* 2023; 37(9): 2451–2471.
35. Han Y. Adaptive control of a class of stochastic nonlinear systems with full state constraints and input saturation using multi-dimensional Taylor network. *Asian J Control* 2022; 24(4): 1609–1621.
36. Han YQ. Adaptive output-feedback tracking control for a class of nonlinear systems with input saturation: a multi-dimensional Taylor network-based approach. *Int J Syst Sci* 2020; 51(13): 2471–2482.
37. Han Y, Li N, He W, et al. Adaptive multi-dimensional Taylor network funnel control of a class of nonlinear systems with asymmetric input saturation. *Int J Adapt Control Signal Process* 2021; 35(5): 713–726.
38. Zhu S, Wang M and Han Y. Adaptive multi-dimensional Taylor network control for nonlinear stochastic systems with time-delay. *Proc IMechE, Part I: J Systems and Control Engineering* 2022; 236(3): 579–591.
39. Li CL, Yan HS and Zhang JJ. Multi-dimensional Taylor network adaptive predictive control for single input single-output nonlinear systems with input time delay. *Trans Inst Meas Contr* 2022; 44(3): 595–608.
40. Yan HS and Kang AM. Tracking control and dynamic regulation of time-varying delay nonlinear systems with actuator saturation via multi-dimensional Taylor networks. *J Franklin Inst* 2020; 357(8): 4759–4778.
41. Qian F, Cai J, Wang B, et al. Adaptive backstepping control for a class of nonlinear systems with unknown time delay. *IEEE Access* 2020; 8: 229–236.
42. Li W, Zhang Z and Ge SS. Stabilization control for strict-feedback nonlinear systems with time delays. *IEEE Trans Syst Man Cybern Syst* 2022; 52(12): 7549–7560.
43. Li S and Hong Y. Adaptive controller design for a class of time-delay nonlinear systems with input saturation. *30th CCC* 2011; 364-369.
44. Psillakis HE and Alexandridis AT. NN-Based adaptive tracking control of uncertain nonlinear systems disturbed by unknown covariance noise. *IEEE Trans Neural Netw* 2007; 18(6): 1830–1835.
45. Liu Z, Lai G, Zhang Y, et al. Adaptive neural control for a class of nonlinear time-varying delay systems with unknown hysteresis. *IEEE Trans Neural Netw Learn Syst* 2014; 25(12): 2129–2140.
46. Li N, Zhu S, He W, et al. Controller design for nonlinear systems subject to both input saturation and asymmetry time-varying state constraints: a novel network-based approach. *Int J Adapt Control Signal Process* 2022; 36(12): 3124–3141.
47. Ma J, Ge SS, Zheng Z, et al. Adaptive NN control of a class of nonlinear systems with asymmetric saturation actuators. *IEEE Trans Neural Netw Learn Syst* 2015; 26(7): 1532–1538.
48. Du Y, Zhu S, Zhai L, et al. Switching threshold-based event-triggered adaptive asymptotic tracking control for stochastic nonlinear systems with full-state constraints. *Int J Robust Nonlinear Control* 2023; 33(13): 7908–7928.
49. Zhang JJ and Yan HS. MTN optimal control of MIMO non-affine nonlinear time-varying discrete systems for tracking only by output feedback. *J Franklin Inst* 2019; 356(8): 4304–4334.
50. He WJ, Zhu SL, Lu LT, et al. Adaptive multi-switching-based global tracking control for switched nonlinear systems with prescribed performance. *IEEE Trans Autom Sci Eng* 2023; 1–10. DOI: 10.1109/TASE.2023.3277470
51. Liu YJ, Tong SC, Wang D, et al. Adaptive neural output feedback controller design with reduced-order observer for a class of uncertain nonlinear SISO systems. *IEEE Trans Neural Netw* 2011; 22(8): 1328–1334.